Selectin−Ligand Interactions Revealed by Molecular Dynamics Simulation in Solution

Hideki Tsujishita,*,† Yasuyuki Hiramatsu,† Noriko Kondo,† Hiroshi Ohmoto,† Hirosato Kondo,† Makoto Kiso,‡ and Akira Hasegawa‡

New Drug Discovery Research Laboratory, Kanebo Ltd., 1-5-90 Tomobuchi-cho, Miyakojima-ku, Osaka 534, Japan, and Department of Applied Bioorganic Chemistry, Gifu University, Gifu 501-11, Japan

Received August 23, 1996[⊗]

Through a computer modeling and simulation technique, we investigated the binding mode of a complex of E-selectin−GSC-150, which is a novel selectin blocker. GSC-150 is the 3′-sulfated Lewis X derivative with a long, branched alkyl chain. Initial attempts to construct a model for E-selectin−GSC-150 complex were performed based on a previously reported model of E-selectin−sialyl Lewis X (sLe^x) complex [Kogan, T. P.; Revelle, B. M.; Tapp, S.; Scott, D.; Beck, P. J. *J. Biol. Chem.* **1995**, *270*, 14047−14055]. In our model, the carbohydrate portion of GSC-150 interacted with the protein in a similar manner as that of sLe^x reported previously. Interestingly, each of the branched alkyl chains extended on the surface of E-selectin and interacted with two different hydrophobic portions. One of these hydrophobic portions consists of Tyr44, Pro46, and Tyr48. Another portion forms a shallow cavity, and it consists of Ala9, Leu114, and the alkyl moieties of the side chains of Lys111, Lys112, and Lys113. A subsequent 200-ps molecular dynamics simulation in solution revealed that the interactions involved in the sugar portion of the ligand were relatively weak, whereas the hydrophobic interactions involved in the branched alkyl chains were fairly stable in solution. These results suggest that the branched alkyl chain serves as an "anchor" for the tight binding of GSC-150 on the surface of E-Selectin. This is the first attempt to evaluate the dynamics of E-Selectin−ligand interactions in solution, and it sheds light on the nature of ligand recognition by selectins.

Introduction

Adhesion of leukocytes to the endothelial cells of blood vessels is a crucial step in the inflammatory response. It is known that several cell adhesion molecules are involved in this process.[1] In particular, selectins play important roles in the early stages.[2] There are three subtypes of selectins: E-selectin (ELAM-1), P-selectin (GMP-140), and L-selectin (LECAM-1). They are expressed on various cell surfaces. For example, E-selectin expression is induced on the surface of endothelial cells, after 4−6 h from the stimulation by inflammatory cytokines. In contrast, P-selectin is rapidly expressed on platelets and endothelial cells upon stimulation by agonists such as thrombin. L-selectin is expressed on leukocytes. The cell−cell interactions mediated by those molecules cause "rolling" of leukocytes in the bloodstream and initiate the extravasation of leukocytes to the site of injury or inflammation. Therefore, the inhibition of cell adhesion involving selectins is an attractive target for the development of new antiinflammatory drugs.

We have recently developed a potent selectin inhibitor, GSC-150 (**2**, Figure 1).[3] This compound is an analog of the natural selectin ligand, sialyl Lewis X (sLe^x; Neu5Acα2−3Galβ1−4[Fucα1−3]GlcNAc; **1**, Figure 1), in which the sialic acid in sLe^x is replaced by a sulfate. The most characteristic part of the structure of GSC-150 is a branched alkyl chain (2-tetradecylhexadecyl; namely "B-30") attached to the 1-position. This branched chain mimics the natural ceramide and significantly contributes to the inhibitory activity of GSC-150. As shown in Table 1, GSC-150 is much more potent than sLe^x. In contrast, a 3′-sulfated analog that lacks B-30 (**3**, Figure 1) shows weaker activity, which is almost equal to that of sLe^x. From these results, it is expected that B-30 plays important roles in binding with selectins.

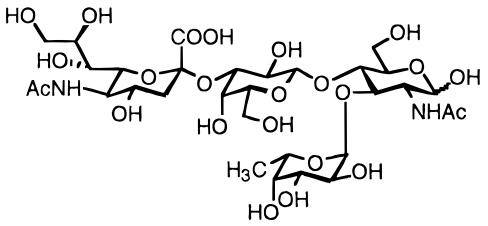

1 (sialyl Lewis X)

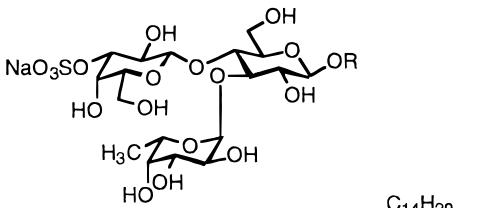

2 (GSC-150): R = $C_{14}H_{29}$ / $C_{14}H_{29}$

3: R = —H

Figure 1. Chemical structures of the selectin ligands.

Selectins are composed of an amino-terminal lectin-like domain followed by an epidermal growth factor (EGF) like domain, a variable number of complement receptor related repeats (CR), a hydrophobic transmembrane domain, and a cytoplasmic region. It is believed

* Author to whom correspondence should be addressed.
† New Drug Discovery Research Laboratory, Kanebo Ltd.
‡ Department of Applied Bioorganic Chemistry, Gifu University.
⊗ Abstract published in *Advance ACS Abstracts,* January 1, 1997.

S0022-2623(96)00610-3 CCC: $14.00

Table 1. Selectin-Blocking Activity of Compounds **1**−**3**[a]

compound[b]	IC_{50} (mM)		
	E-selectin	P-selectin	L-selectin
1 (sLe^x)	0.60	>1.0	>1.0
2 (GSC-150)	0.28	0.10	0.03
3	>1.0	0.30	>1.0

[a] Data were taken from ref 3. [b] Compound numbers correspond to those in Figure 1.

that the lectin-like domain contacts various selectin ligands. Recently, the crystal structure of the lectin/EGF-like domains of E-selectin has been resolved.[4] This work revealed that the lectin-like domain of E-selectin exhibits almost the same fold as rat mannose-binding protein.[5,6] Although the precise structure of E-selectin−sLe^x complex has not been resolved yet, many groups have tried to investigate its interaction modes in experimental or theoretical ways.[4,7−18] From the similarity with rat mannose-binding protein, it is believed that the hydroxyl groups of the fucose in sLe^x coordinate to a calcium ion bound on E-selectin, which is critical to ligand recognition by the protein.[9] Furthermore, a hydroxyl group on fucose would also form hydrogen bonds with the side chains of Glu80 and Asn82, both of which coordinate to the calcium ion. The negative charge on the ligands, which is also critical to ligand recognition,[11,18] has been believed to interact with Lys113 on E-selectin.[4,13] Recently, Kogan et al.[16] have reported another structural model of the complex of E-selectin−sLe^x. Surprisingly, they presented in their paper that mutants of E-selectin, in which Lys113 was replaced by either a neutral glutamine or an acidic glutamate, retained binding activity to the ligands. On the basis of this result, they selected Arg97, which is another critical basic residue on E-selectin, as the counterpart for the carboxylate on sLe^x. Another notable interaction in their model is a hydrogen bond between the 6-hydroxyl group on galactose and the phenol of Tyr94.

Since the carbohydrate portion of GSC-150 is almost the same as that of sLe^x, the binding mode of this sugar portion may be acceptable in the model reported by Kogan et al. However, the interaction mode between the B-30 portion of GSC-150 and E-selectin is completely unclear. As mentioned above, B-30 is crucial to enhance the inhibitory activity of GSC-150 (Table 1). Therefore, it is very important to explore the detailed interactions between B-30 and the protein. In this paper, we describe a suitable structural model of GSC-150−E-selectin complex. The binding site of B-30 to E-selectin was explored by conformational analysis, using a high-temperature molecular dynamics (MD) method, a well-established technique to explore the conformational space of a molecule.[19] In this work, we also analyzed the dynamics of the structure of the complex using a 200-ps MD simulation, including explicit solvent water. This is the first reported attempt to evaluate the dynamics of selectin−ligand interactions in solution. The explicit consideration of the solvent is necessary because B-30 might interact with the protein through hydrophobic forces. Furthermore, since carbohydrates have a fairly hydrophilic nature, inclusion of the solvent is needed to understand the modes of selectin−carbohydrate-containing ligand interactions.

Computational Methods

All of the calculations were performed using AMBER 4.0[20] with the force field published by Cornell et al.[21] The force-field parameters for the carbohydrate portion of GSC-150 were derived from GLYCAM_93, a general force field for carbohydrates that is suitable to AMBER, which takes account of the exoanomeric effect.[22] The parameters for the calcium ion were taken from Hamaguchi et al.[23] and Maynard et al.[24] The parameters for the sulfate were taken from Huige and Altona.[25] Graphic manipulations and representations were performed by MidasPlus 2.0.[26]

Model Construction. The crystal structure of the lectin-like domain of E-selectin was obtained from the Protein Data Bank (ident code: 1ESL). The model building for the carbohydrate portion of GSC-150 was based on the model of the complex of E-selectin−sLe^x proposed by Kogan et al.[16] That is, the carbohydrate structure of GSC-150 was constructed using the glycosidic torsion angles suggested by Ichikawa et al.[27] and Cooke et al.,[10] which were derived from the NMR analysis of sLe^x with soluble E-selectin. The initial structure of GSC-150 was then placed on E-selectin. Consequently, the 2- and 3-OH groups on fucose were coordinated to the calcium, and the sulfate on the ligand was directed to Arg97 and to another adjacent basic amino acid, Lys99. At this step, we directed the alkyl chains of B-30 to the solvent region, in order to avoid any artificial interactions with the protein. The constructed model was then minimized until the root mean square of the gradients was below 0.05 kcal/(mol·Å). The coordinates of the protein were fixed during the calculation. In the minimization, we used a distance-dependent dielectric constant, $\epsilon = 4r$, to include the solvent effect implicitly.

In order to determine the bound conformation of the B-30 portion of the ligand, we performed a high-temperature MD calculation. The calculation was performed for 100 ps with an integral time step of $\Delta t =$ 1 fs. Only the B-30 portion was allowed to move during the calculation. The temperature of the system was maintained at 900 K using Berendsen's weak coupling algorithm.[28] During the MD calculation, all of the bond lengths were fixed by SHAKE algorithm.[29] Then we collected several low-energy conformers appearing in the resultant trajectory and evaluated each of them on a graphic device. Consequently, we found an interesting conformation in which each of the two alkyl chains extended along two distinct hydrophobic surfaces on E-selectin (see below). We chose this conformation as the initial model of the complex and minimized it until the root mean square of the gradients was below 0.05 kcal/(mol·Å). The coordinates of the protein were fixed during the calculation. A distance-dependent dielectric constant, $\epsilon = 4r$, was used again.

Simulation of the Complex in Solution. The model of the complex was solvated by the addition of 1238 TIP3P water molecules[30] within 25 Å from the 1-oxygen of glucose in GSC-150. The water molecules were then minimized until the root mean square of the gradients was below 0.05 kcal/(mol·Å). Following the minimization, the water molecules were equilibrated by a 5-ps MD calculation at a temperature of 298 K. An integral time step of $\Delta t = 2$ fs was used. After that, all of the water molecules, the ligand, and the residues in

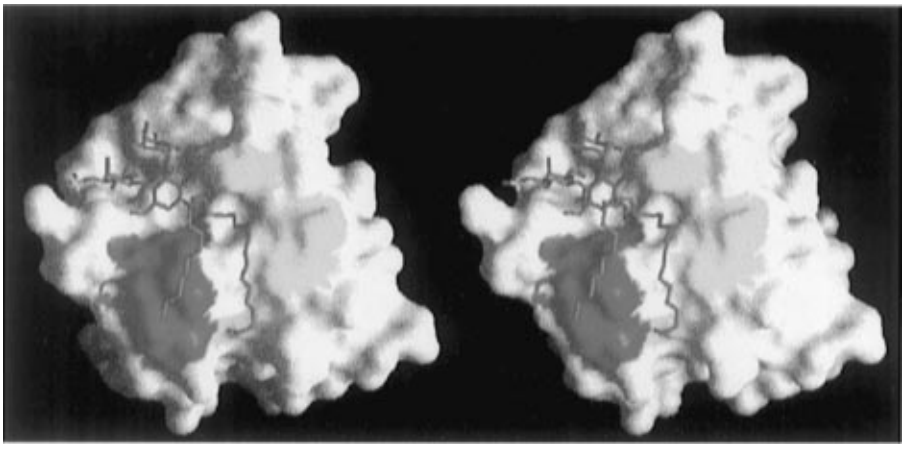

Figure 2. Stereorepresentation of the initial model of the lectin domain of E-selectin−GSC-150 complex. The structure of the ligand is represented by the green cylinder model. The structure of the protein is represented by surface model. One of the two hydrophobic surfaces (Tyr44, Pro46, Tyr48) is colored by magenta, and another (the alkyl moieties of the side chains of Lys111, Lys112, Lys113, Ala9, and Leu114) is colored by yellow. The picture was created by GRASP software.[38]

the ligand-binding site on the protein (Ser6−Met10, Ser43−Tyr49, Trp76−Arg84, Val91−Val101, Trp104−Ala115, and the calcium ion) were minimized until the root mean square of the gradients was below 0.05 kcal/(mol·Å). Part of the system was then subjected to a 200-ps MD simulation at a temperature of 298 K. An integral time step of $\Delta t = 2$ fs was used. The coordinates of the system were recorded at every 0.2 ps during the calculation, for the following analyses of the trajectory. In the calculations with the explicit water, a dielectric constant, $\epsilon = 1$, was used. During the MD calculations, all of the bond lengths were fixed by SHAKE algorithm. A nonbonded cutoff of 9 Å was used in all of the above calculations.

Analyses of the Trajectory. Various analyses of the trajectory from the MD calculation in solution were performed with several in-house programs. For the interactions observed in the initial model complex, we calculated the distances of each interaction from the sets of coordinates in the trajectory. The analysis of bound waters (see below) was done as follows: the 200-ps-long trajectory was first divided into 20 10-ps-long "windows". For each set of coordinates in an individual window, we searched all water molecules and determined which waters could form hydrogen bonds with both the ligand and the protein. For each atom pair, we treated it as hydrogen bonding when the distance between the heavy atoms in the donor, and the acceptor was within 3.5 Å and the angle formed by the acceptor atom, hydrogen of the donor, and the heavy atom of donor was in the range 90−180°. The distances of hydrogen bonds were fluctuating around a nominal hydrogen-bond distance in the dynamics simulation. Therefore we used a rather long distance threshold in the hydrogen-bond analysis. For the analysis of the behavior of the B-30 portion (see below), we calculated the "ratio of hidden surface area" as a measure of hydrophobic interactions with the protein. This indicator was calculated in the following way: for each set of coordinates in the trajectory, we calculated the solvent-accessible surface area of the B-30 portion. The area calculations were performed in two ways: one was the area of free B-30 (A_{free}), which was calculated after the deletion of the protein coordinates. The other was the area of bound B-30 ($A_{complex}$), calculated in the presence of the protein. Then, the ratio of hidden surface area was calculated by the following equation:

$$\text{ratio of hidden surface area (\%)} = (A_{free} - A_{complex})/A_{free} \times 100$$

As indicated by the above equation, the ratio of hidden surface area is the ratio of the solvent accessible surface area of B-30 that was buried in the protein. A larger percentage of hidden surface area reflects wider B-30 contacts with the protein surface. The calculation of solvent-accessible surface area was done by the methods of Richmond[31] and Wesson and Eisenberg.[32] Hydrogen atoms were not included in the calculation.

Results

The initial attempt at docking the carbohydrate portion in GSC-150 on E-selectin produced almost the same interaction mode as those observed in the previously reported complex model of sLe^x−E-selectin.[16] That is, the 2- and 3-hydroxyl groups on the fucose coordinated to the calcium ion bound on E-selectin. The 3-hydroxyl groups also formed hydrogen bonds with the amide nitrogen and the carboxylate on the side chains of Asn82 and Glu80, respectively. The sulfate on the ligand formed ion pairs with two basic residues, Arg97 and Lys99. In addition, the 6-hydroxyl group on galactose formed a hydrogen bond with the hydroxyl group on the phenol ring of Tyr94.

Next, we explored the B-30 binding site to E-selectin by conformational analysis using the high-temperature MD technique. Through this calculation, we extracted several low-energy conformers. Among those conformers, we found an interesting one in which each of the two alkyl chains extended along two different hydrophobic surfaces on E-selectin. As indicated in Figure 2, one of those hydrophobic surfaces consists of Tyr44, Pro46, and Tyr48. Another surface forms a shallow cavity, and it consists of Ala9, Leu114, and the alkyl moieties of the side chains of Lys111, Lys112, and Lys113.

Figure 3 summarizes the interactions between the ligand and E-selectin observed after the minimization of our constructed model. In addition to the interactions described above, the 2-OH of the glucose formed hydrogen bonds with the carboxylate and the amino group of Glu107 and Lys111, respectively. sLe^x could not form

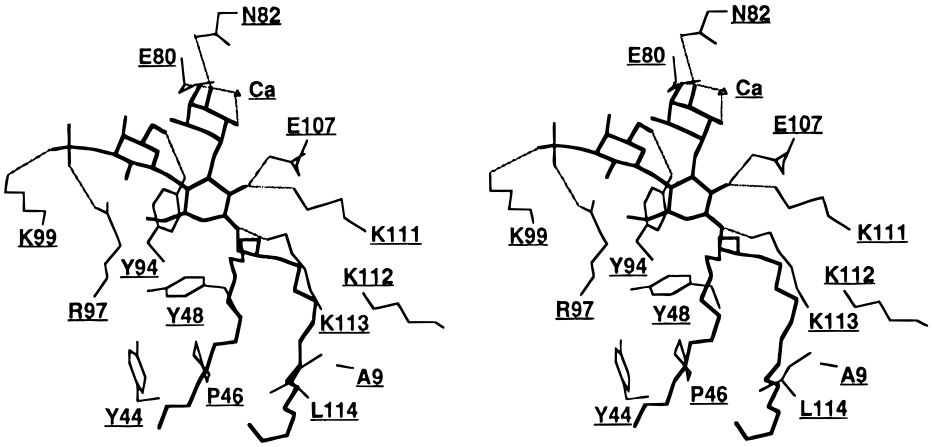

Figure 3. Stereorepresentation of the initial model of E-selectin−GSC-150 complex. The structure of the ligand is represented by thick lines. The protein is indicated by thin lines. For clarity, only the residues of the protein that interact with the ligand are shown. Gray, thin lines indicate the interactions between the protein and the ligand.

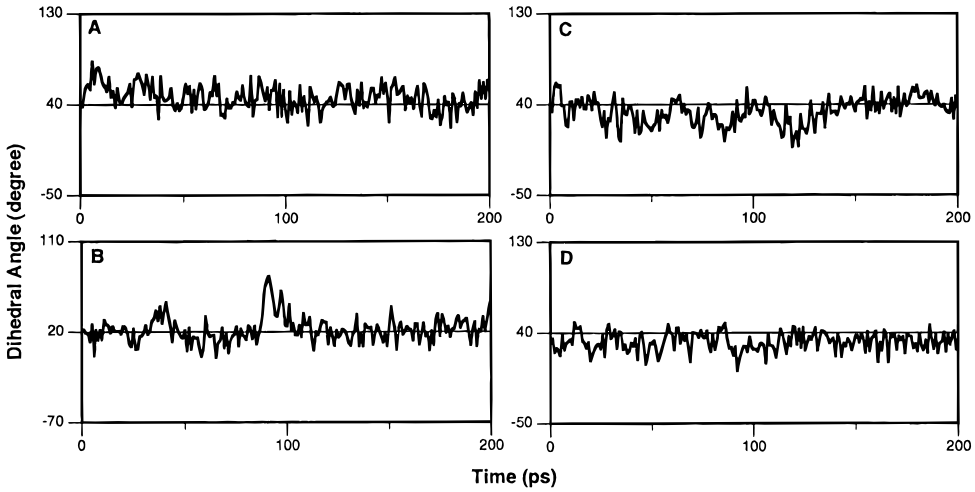

Figure 4. Change of the glycosidic torsion angles of GSC-150 in the complex model during the simulation in solution. A, ϕ angle of Gal−Glc; B, ψ angle of Gal−Glc; C, ϕ angle of Fuc−Glc; D, ψ angle of Fuc−Glc.

such interactions because the 2-position of the glucose is replaced by an *N*-acetylamide group. Moreover, the 1-oxygen of the glucose formed a hydrogen bond with Lys113. The conformation of the trisaccharides in GSC-150 was similar to that of sLe^x bound on E-selectin, as determined by the NMR experiments.[10] The glycosidic torsion angles of GSC-150 were Gal−Glc, 44/21, and Fuc−Glc, 53/24. These values were comparable to the predicted values of sLe^x bound to E-selectin: Gal−GlcNAc, 55/7, and Fuc−GlcNAc, 48/25.

After the construction of the model complex, we subjected the model to a 200-ps MD simulation containing explicit water solvent and evaluated the dynamic behavior of the model in solution. Figure 4 indicates the change of the glycosidic torsion angles of GSC-150 during the MD simulation. The averages and standard deviations of these values were Gal−Glc, 47 ± 12/22 ± 13, and Fuc−Glc, 34 ± 13/32 ± 9. These values indicate that the sugar portions of the ligand retained almost the same conformation as in the initial model. However, significant fluctuations were observed for the ψ angle of Gal−Glc (Figure 4B) and the ϕ angle of Fuc−Glc (Figure 4C). These fluctuations would reflect some changes in the interactions between GSC-150 and the protein.

Next, we monitored the distances of the plausible interactions observed in the initial model complex during the simulation. Figure 5 shows the distances between each atom as a function of simulation time. The 3′-sulfate group of GSC-150 interacted with both Arg97 and Lys99 in the initial model. However, both interactions were broken in the early stage of the calculation (Figure 5A). Moreover, the sulfate moved far from the protein at about 90 ps. This conformational change might correspond to the fluctuation of the ψ glycosidic torsion angle for Gal−Glc observed at that time (Figure 4B). The same tendency was observed for the interaction between the 6-OH on the galactose and Tyr94. In the initial model, the 6-OH on the galactose formed a hydrogen bond with the hydroxyl group on Tyr94, with a distance of 3.0 Å. This interaction became weaker during the simulation, and its distance fluctuated in the range from 5 to 9 Å.

In the initial complex model, the 2- and 3-OH groups on the fucose of GSC-150 coordinated to the calcium ion bound on E-selectin, with distances of 3.1 and 2.8 Å, respectively. The fucose−calcium interactions of fucosylated ligands are believed to be critical in the binding to E-selectin. Figure 5B shows the changes of the distances of the fucose−calcium interaction during the simulation in solution. As indicated in Figure 5B, the coordination of the 3-OH on fucose to the calcium was very stable. In contrast, the coordination of the 2-OH was rather weak, and the distance of the interaction

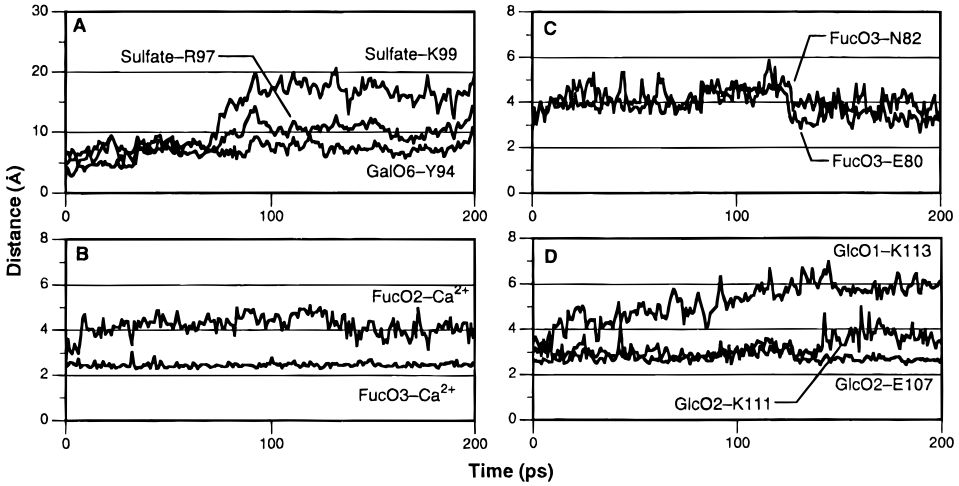

Figure 5. Change of the distances of the interactions between E-selectin and GSC-150 during the simulation in solution. Each part indicates the following: A, the interactions involved in the sulfate and the galactose; B, the interactions between the fucose and calcium; C, the interactions between the fucose and the protein; D, the interactions involved in the glucose.

fluctuated in the range from 3 to 5 Å. In the initial model, the 3-OH of fucose also participated in hydrogen bonds with the side chains of Glu80 and Asn82. These interactions were not very stable in solution until about 120 ps (Figure 5C). After this point, however, the 3-OH of fucose slightly moved toward the protein and the hydrogen bonds became more stable. This would affect the dynamic behavior of the Fuc−Glc glycosidic linkage (Figure 4C) described above.

Figure 5D indicates the changes of the distances between the glucose portion of GSC-150 and the protein during the simulation. In the initial complex model, the 2-OH of the glucose formed two hydrogen bonds with the amino group of Lys111 and the carboxylate of Glu107. In contrast to the other interactions involved in the sugar portion of the ligand, those two hydrogen bonds were rather strong and stable. For the hydrogen bond with Lys111, however, the amplitude of the fluctuation of its distance became larger at about 150 ps, which indicates that the interaction became rather unstable. For the glucose portion, a hydrogen bond between the 1-OH of the glucose and the amino group of Lys113 was also observed in the initial model. However, this bond was broken in the early stage of the simulation.

There were evidences that some of the lectin−ligand binding modes contain indirect interactions via bound waters.[33] Therefore, we evaluated the presence of this type of interaction mediated by water molecules in the simulation in solution (Figure 6). As shown in Figure 6, there were no waters that tightly interacted with both the ligand and the protein over the whole simulation period. For the last 100 ps, we detected a water molecule around the 2-OH of the glucose, the carboxylate of Glu107, and the amino group of Lys113. Since the carboxylate of Glu107 interacted directly with the 2-OH of the glucose during this period (Figure 5D), that water would not mediate the interaction between these atoms. On the other hand, the 2-OH of the glucose and the amino group of Lys113 did not bind directly to each other duirng that simulation period (data not shown). Therefore this result strongly suggests that the bound water molecule would mediate the indirect interaction between the 2-OH of the glucose and the amino group of Lys113 for the last 100 ps. Figure 7 shows this more

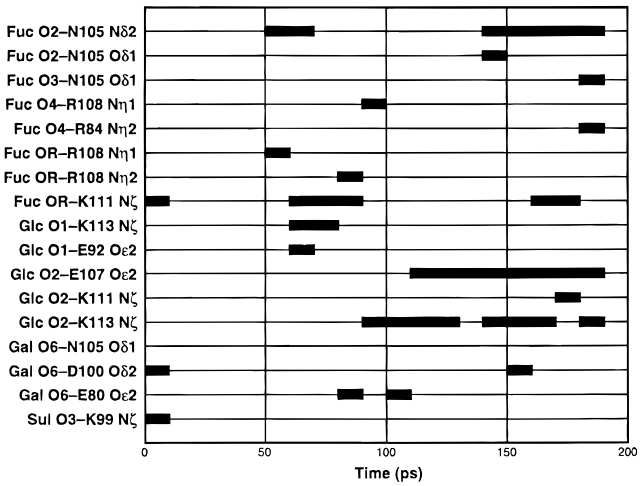

Figure 6. Water-mediated interactions between E-selectin and GSC-150 observed in the simulation in solution. Bold lines indicate the simulation periods when water-mediated interactions were observed between the protein−ligand pairs shown at the left side of the figure.

clearly. In the snapshot at 150 ps (Figure 7C), we could see the water molecule interacting with the 2-OH of the glucose and Lys113. In the early portion of the simulation, this water was located far from Lys113 and was moving around the solute (Figure 7A,B). Near 100 ps, this water was then trapped by the protein and was kept fixed until almost the end of the simulation.

Next we analyzed the behavior of the branched alkyl chain (B-30) portion in GSC-150 during the simulation in solution. The initial complex model suggested that the two alkyl chains in the B-30 portion of the ligand would make hydrophobic interactions with the hydrophobic portions on the protein. Since direct estimation of the hydrophobic force is difficult, we used the ratio of the solvent accessible surface area of B-30 that was hidden by the protein as an indication of the strength of the hydrophobic interaction (see Methods section). Figure 8 indicates the ratio of the hidden surface area of each alkyl chain as a function of the simulation time. For the alkyl chain that was buried in the cavity consisting of the alkyl side chains of Lys111, Lys112, Lys113, Ala9, and Leu114 (namely, the A chain), its hidden surface area retained the initial value and fluctuated minimally (Figure 8A). This suggests that

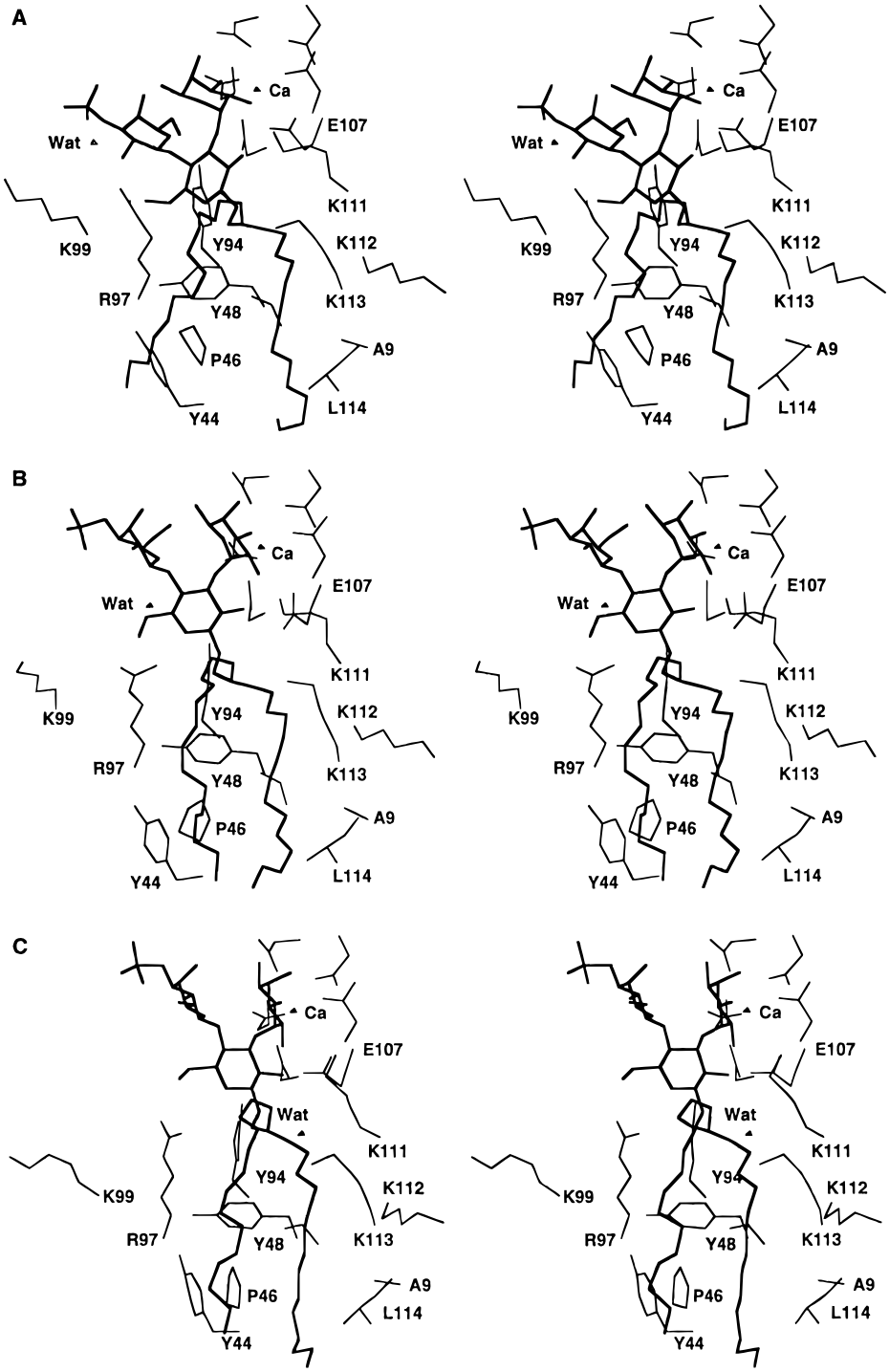

Figure 7. Stereorepresentations of the snapshots of the E-selectin−GSC-150 complex model at (A) 0 ps, (B) 50 ps, and (C) 150 ps during the simulation in solution. The structure of GSC-150 is indicated by thick lines. Thin lines indicate the structure of E-selectin. For clarity, only the residues in the ligand-binding site on the protein are shown. A triangle labeled as "Wat" represents the water molecule that mediated the interaction between 2-OH of the glucose and Lys113 for the last 100 ps (see Figure 6).

the A chain interacted tightly with the hydrophobic cavity on the protein. On the other hand, the hidden area of the alkyl chain on the surface of Tyr44, Pro46, and Tyr48 (namely, the B chain) fluctuated greatly during the simulation (Figure 8B). This is consistent with the interaction involved in the B chain being less stable than that of the A chain. However, since the hidden surface area of the B chain retained more than half of the initial value (Figure 8B), the hydrophobic interaction between this chain and the protein still existed and did not completely disappear. The snapshots of the trajectory show the stability of the interactions involved in B-30 (Figure 7). As shown in Figure 7, while the carbohydrate portion of GSC-150 gradually drifted far away from the surface of E-selectin, B-30 existed at almost the same place during the simulation and interacted tightly with the protein.

Discussion

Our theoretical model for a GSC-150−E-selectin complex suggests that the sugar portion of GSC-150 could interact with E-selectin in a manner similar to that of sLe^x, as proposed by Kogan et al.[16] Moreover, we found that the branched alkyl chains involved in

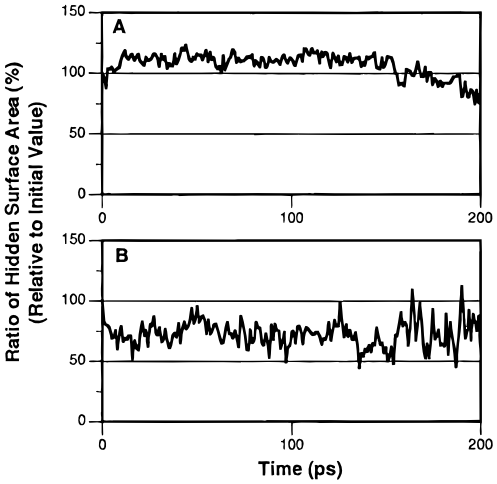

Figure 8. Change of the ratio of hidden surface area of B-30 portion in GSC-150 during the simulation in solution: A, the ratio of the alkyl chain that was buried in the cavity consisting of Lys111, Lys112, Lys113, Ala9, and Leu114 (A chain); B, the ratio of the alkyl chain on the surface of Tyr44, Pro46, and Tyr48 (B chain). Values relative to those in the initial model are shown.

GSC-150 (B-30) could have strong interactions with the hydrophobic portions of E-selectin. It was surprising that E-selectin has such hydrophobic portions on its surface that were suitable for the binding of B-30, although their native roles are still unknown.

The subsequent MD simulation including explicit solvent suggested the difference in the dynamics of the carbohydrate and B-30 portions in GSC-150: the sugar portion rapidly dissociated from E-selectin, while the B-30 portion interacted tightly with the protein. The rapid dissociation of carbohydrate ligands from selectins is a prerequisite for the role of selectins in the inflammatory process.[1,34,35] Selectins interact with leukocytes flowing in the bloodstream and cause their rolling on the blood vessel. For efficient rolling, rapid association/dissociation of selectin−ligand interactions are required. The observed behavior of the carbohydrate portions in GSC-150 might be consistent with the characteristics of natural selectin ligands. The rapid dissociation observed in the sugar portion would be due to the hydrophilic nature of the carbohydrate structure and the environment in the ligand-binding site on E-selectin. On the lectin domain of E-selectin, there are no deep cavities in which ligands could enter. Therefore, when a ligand interacts with E-selectin, there are many solvent water molecules around the ligand binding site. Water solvent has competitive and shielding effects on hydrogen bonding and electrostatic interactions. Such types of interactions involved in the ligand−selectin complex would be affected and weakened by the presence of surrounding water.

Although rapid dissociation is required for native selectin−ligand interactions, it is not preferable for selectin inhibitors. For the potential inhibition of the ligand−selectin interaction, more stable interactions between inhibitors and selectins are required. Our present results suggest that the introduction of hydrophobic moieties to ligands would stabilize ligand−selectin interactions. Our results suggested that the hydrophobic interaction between B-30 in GSC-150 and E-selectin was quite stable in solution. The hydrophobic interaction is a type of aggregation in which the hydrophobic surfaces of molecules interact with each other in the presence of water. For such interactions, an environment surrounded by water, like the ligand-binding site on E-selectin, would be preferable. In such an environment, the B-30 portion serves as an "anchor" in the binding of GSC-150 on the surface of E-selectin.

Recently, Revelle et al.[36] have reported a surprising result that mutants of E-selectin, in which Arg97 was replaced by Asp or Ser, retained their binding ability to ligands. This result makes it difficult to predict the ligand binding site on E-selectin. Many previous reports have proposed models of sLe^x −E-selectin complex in which the negative charge on the ligand interacted with Lys113.[4,13] On the other hand, Kogan et al.[16] have presented a model in which the counterpart of the negative charge on the ligand was Arg97. We adopted Kogan's model in the initial model of the complex of GSC-150−E-selectin. Additionally, we also tried to construct a complex model based on the other model of sLe^x −E-selectin complex. In this case, however, we failed to detect any suitable binding sites for B-30 in GSC-150 (data not shown). Furthermore, Manning et al.[37] have presented a result that supports Kogan's proposal for the ligand binding site on E-selectin. They found that the substitution with the sulfate group at the 6′ positions of galactose in $Lewis^a$ derivatives disrupts the binding to E-selectin. In their paper, they discussed the consistency of the two models with their result. In Kogan's model, the 6′ position of the galactose is directed toward the negatively charged Glu80 and Asp100. Therefore, a substitution with an acidic sulfate group at the 6' position would cause electrostatic repulsion. On the other hand, the 6′ position of the galactose is directed toward Lys111 in another model. If the latter model is true, the sulfation of the 6′ position should stabilize the ligand−selectin interaction. On the basis of these facts, regarding the disruption of E-selectin binding by the sulfation of the 6' position, Manning et al. concluded that Kogan's model would be more reasonable.

Although there is evidence that can rationalize Kogan's model of E-selectin− sLe^x complex, the counterpart of the negative charge on the ligand still remains unknown. On the other hand, this negative charge is believed to be necessary for the binding to E-selectin.[18] Revelle et al.[36] have argued that the interaction between selectins and the negative charge on the ligands might be mediated through water molecules. In this paper, we searched for such bound water molecules during the MD in solution (Figure 6). Through this analysis, we detected a bound water around the 2-OH on the glucose of GSC-150. However, we could not find any bound water molecules that could mediate the interaction between the negative charge on the ligand and E-selectin. The interactions of water molecules with the solute could exist for a very short period. In order to explore the roles of the negative charges on selectin ligands, further calculations, such as a simulation using some selectin mutants, might be needed.

Lastly, we are now investigating the structure−activity relationship concerning the B-30 portion, i.e., the length of the alkyl chain and so on. In our model of the GSC-150 complex, each of the two alkyl chains in B-30 interacted with two distinct hydrophobic surfaces on the protein, and the lengths of the chains seemed to

be critical. Therefore, we think that the alkyl chain must be branched and that the sizes of the chains in B-30 would be optimized for the best binding affinity of the ligand. We are now synthesizing and testing several analogs to confirm our hypothesis. These results will be reported elsewhere.

Acknowledgment. We thank Prof. Shuichi Hirono (Kitasato University, Tokyo, Japan) for helpful discussions and critical reading of the manuscript.

References

(1) Springer, T. A. Traffic Signals for Lymphocyte Recirculation and Leukocyte Emigration: The Multiship Paradigm. *Cell* **1994**, *76*, 301−314.
(2) Lasky, L. A. Selectins: Interpreters of Cell-Specific Carbohydrate Information During Inflammation. *Science* **1992**, *258*, 964−969.
(3) Wada, Y.; Saito, T.; Matsuda, N.; Ohmoto, H.; Yoshino, K.; Ohashi, M.; Kondo, H.; Ishida, H.; Kiso, M.; Hasegawa, A. Studies on Selectin Blockers. 2. Novel Selectin Blocker as Potential Therapeutics for Inflammatory Disorders. *J. Med. Chem.* **1996**, *39*, 2055−2059.
(4) Graves, B. J.; Crowther, R. L.; Chandran, C.; Rumberger, J. M.; Li, S.; Huang, K.-S.; Presky, D. H.; Familletti, P. C.; Wolitzky, B. A.; Burns, D. K. Insight into E-selectin/Ligand Interaction from the Crystal Structure and Mutagenesis of the Lec/EGF Domains. *Nature* **1994**, *367*, 532−538.
(5) Weis, W. I.; Kahn, R.; Fourme, R.; Drickamer, K.; Hendrickson, W. A. Structure of the Calcium-Dependent Lectin Domain from a Rat Mannose-Binding Protein Determined by MAD Phasing. *Science* **1991**, *254*, 1608−1615.
(6) Weis, W. I.; Drickamer, K.; Hendrickson, W. A. Structure of a C-Type Mannose-Binding Protein Complexed with an Oligosaccharide. *Nature* **1992**, *360*, 127−134.
(7) Bajorath, J.; Hollenbaugh, D.; King, G.; Harte, W., Jr.; Eustice, D. C.; Darveau, R. P.; Aruffo, A. CD62/P-selectin Binding Sites for Myeloid Cells and Sulfatides Are Overlapping. *Biochemistry* **1994**, *33*, 1332−1339.
(8) Blanck, O.; Iobst, S. T.; Gabel, C.; Drickmer, K. Introduction of Selectin-Like Binding Specificity into a Homologous Mannose-Binding Protein. *J. Biol. Chem.* **1996**, *271*, 7289−7292.
(9) Brandley, B. K.; Kiso, M.; Abbas, S.; Nikrad, P.; Srivasatava, O.; Foxall, C.; Oda, Y.; Hasegawa, A. Structure-Function Studies on Selectin Carbohydrate Ligands. Modifications to Fucose, Sialic Acid and Sulphate as a Sialic Acid Replacement. *Glycobiology* **1993**, *3*, 633−639.
(10) Cooke, R. M.; Hale, R. S.; Lister, S. G.; Shah, G.; Weir, M. P. The Conformation of the Sialyl Lewis X Ligand Changes upon Binding to E-selectin. *Biochemistry* **1994**, *33*, 10591−10596.
(11) DeFrees, S. A.; Gaeta, F. C.; Lin, Y.-C.; Ichikawa, Y.; Wong, C.-H. Ligand Recognition by E-selectin: Analysis of Conformation and Activity of Synthetic Monomeric and Bivalent Sialyl Lewis X Analogs. *J. Am. Chem. Soc.* **1993**, *115*, 7549−7550.
(12) Erbe, D. V.; Watson, S. R.; Presta, L. G.; Wolitzky, B. A.; Foxall, C.; Brandley, B. K.; Lasky, L. A. P- and E-selectin Use Common Sites for Carbohydrate Ligand Recognition and Cell Adhesion. *J. Cell. Biol.* **1993**, *120*, 1227−1235.
(13) Erbe, D. V.; Wolitzkey, B. A.; Presta, L. G.; Norton, C. R.; Ramos, R. J.; Burns, D. K.; Rumberger, J. M.; Rao, B. N. N.; Foxall, C.; Brandley, B. K.; Lasky, L. A. Identification of an E-selectin Region Critical for Carbohydrate Recognition and Cell Adhesion. *J. Cell. Biol.* **1992**, *119*, 215−227.
(14) Hollenbaugh, D.; Aruffo, A.; Senter, P. D. Effects of Chemical Modification on the Binding Activities of P-selectin Mutants. *Biochemistry* **1995**, *34*, 5678−5684.
(15) Hollenbaugh, D.; Bajorath, J.; Stenkamp, R.; Aruffo, A. Interaction of P-selectin (CD62) and Its Cellular Ligand: Analysis of Critical Residues. *Biochemistry* **1993**, *32*, 2960−2966.
(16) Kogan, T. P.; Revelle, B. M.; Tapp, S.; Scott, D.; Beck, P. J. A Single Amino Acid Residue Can Determine the Ligand Specificity of E-selectin. *J. Biol. Chem.* **1995**, *270*, 14047−14055.
(17) Scheffler, K.; Ernst, B.; Katopodis, A.; Magnani, J. L.; Wang, W. T.; Weisemann, R.; Peters, T. Determination of the Bioactive Conformation of the Carbohydrate Ligand in the E-selectin/Sialyl Lewis^x Complex. *Angew. Chem., Int. Ed. Engl.* **1995**, *34*, 1841−1844.
(18) Tyrrell, D.; James, P.; Rao, N.; Foxall, C.; Abbas, S.; Dasgupta, F.; Nashed, M.; Hasegawa, A.; Kiso, M.; Asa, D.; Kidd, J.; Brandley, B. K. Structural Requirements for the Carbohydrate Ligand of E-selectin. *Proc. Natl. Acad. Sci. U.S.A.* **1991**, *88*, 10372−10376.
(19) Bruccoleri, R. E.; Karplus, M. Conformational Sampling Using High-Temperature Molecular Dynamics. *Biopolymers* **1990**, *29*, 1847−1862.
(20) Pearlman, D. A.; Case, D. A.; Caldwell, G. L.; Seibel, G. L.; Singh, U. C.; Weiner, P.; Kollman, P. A. (1991) AMBER 4.0, University Of California, San Francisco.
(21) Cornell, W. D.; Cieplak, P.; Bayly, C. I.; Gould, I. R.; Merz, K. M., Jr.; Ferguson, D. M.; Spellmeyer, D. C.; Fox, T.; Caldwell, J. W.; Kollman, P. A. A Second Generation Force Field for the Simulation of Proteins, Nucleic Acids, and Organic Molecules. *J. Am. Chem. Soc.* **1995**, *117*, 5179−5197.
(22) Woods, R. J.; Dwek, R. A.; Edge, C. J.; Fraser-Reid, B. Molecular Mechanical and Molecular Dynamical Simulations of Glycoproteins and Oligosaccharides. 1. GLYCAM_93 Parameter Development. *J. Phys. Chem.* **1995**, *99*, 3832−3846.
(23) Hamaguchi, N.; Charifson, P.; Darden, T.; Xiao, L.; Padmanabhan, K.; Tulinsky, A.; Hiskey, R.; Pedersen, L. Molecular Dynamics Simulation of Bovine Prothrombin Fragment-1 in the Presence of Calcium Ions. *Biochemistry* **1992**, *31*, 8840−8848.
(24) Maynard, A. T.; Eastman, M. A.; Darden, T.; Deerfield, D. W. I.; Hiskey, R. G.; Pedersen, L. Effect of Calcium (II) and Magnesium (II) Ions on the 18−23 γ-Carboxyglutamic Acid Containing Cyclic Peptide Loop of Bovine Prothrombin. An AMBER Molecular Mechanics Study. *Int. J. Pept. Protein Res.* **1988**, *31*, 137−149.
(25) Huige, C. J. M.; Altona, C. Force Field Parameters for Sulfates and Sulfamates Based on Ab Initio Calculations: Extensions of AMBER and CHARMm Fields. *J. Comput. Chem.* **1995**, *16*, 56−79.
(26) Ferrin, T. E.; Huang, C. C.; Jarvis, L. E.; Langridge, R. The MIDAS Display System. *J. Mol. Graphics* **1988**, *6*, 13−27.
(27) Ichikawa, Y.; Lin, Y.-C.; Dumas, D. P.; Shen, G.-J.; Garcia-Junceda, E.; Williams, M. A.; Bayer, R.; Ketcham, C.; Walker, L. E.; Paulson, J. C.; Wong, C.-H. Chemical-Enzymatic Synthesis and Conformational Analysis of Sialyl Lewis X and Derivatives. *J. Am. Chem. Soc.* **1992**, *114*, 9283−9298.
(28) Berendsen, H. J. C.; Postma, J. P. M.; van Gunsteren, W. F.; DiNola, A.; Haak, J. R. Molecular Dynamics with Coupling to an External Bath. *J. Chem. Phys.* **1984**, *81*, 3684−3690.
(29) van Gunsteren, W. F.; Berendsen, H. J. C. Algorithms for Macromolecular Dynamics and Constraint Dynamics. *Mol. Phys.* **1977**, *34*, 1311−1327.
(30) Jorgensen, W. L.; Chandrasekhar, J.; Madura, J.; Impey, R. W.; Klein, M. L. Comparison of Simple Potential Functions for Simulating Liquid Water. *J. Chem. Phys.* **1983**, *79*, 926−935.
(31) Richmond, T. J. Solvent Accessible Surface Area and Excluded Volume in Proteins. *J. Mol. Biol.* **1984**, *178*, 63−89.
(32) Wesson, L.; Eisenberg, D. Atomic Solvation Parameters Applied to Molecular Dynamics of Proteins in Solution. *Protein Sci.* **1992**, *1*, 227−235.
(33) Bourne, Y.; van Tilbeurgh, H.; Cambillau, C. Protein-Carbohydrate Interactions. *Curr. Opin. Struct. Biol.* **1993**, *3*, 681−686.
(34) Lawrence, M. B.; Springer, T. A. Leukocytes Roll on a Selectin at Physiologic Flow Rates: Distinction from and Prerequisite for Adhesion Through Integrins. *Cell* **1991**, *65*, 859−873.
(35) Ushiyama, S.; Laue, T. M.; Moore, K. L.; Erickson, H. P.; McEver, R. P. Structural and Functional Characterization of Monomeric Soluble P-selectin and Comparison with Membrane P-selectin. *J. Biol. Chem.* **1993**, *268*, 15229−15237.
(36) Revelle, B. M.; Scott, D.; Kogan, T. P.; Zheng, J.; Beck, P. J. Structure-Function Analysis of P-selectin-Sialyl Lewis^x Binding Interactions. Mutagenic Alteration of Ligand Binding Specificity. *J. Biol. Chem.* **1996**, *271*, 4289−4297.
(37) Manning, D. D.; Bertozzi, C. R.; Pohl, N. L.; Rosen, S. D.; Kiessling, L. L. Selectin-Saccharide Interactions: Revealing Structure-Function Relationships with Chemical Synthesis. *J. Org. Chem.* **1995**, *60*, 6254−6255.
(38) Nicolls, A.; Sharp, K. A.; Honig, B. Protein Folding and Association: Insights from the Interfacial and Thermodynamic Properties of Hydrocarbons. *Proteins Struct. Funct. Genet.* **1991**, *11*, 281−296.

JM9606103